Electronic Supplementary Material (ESI) for Lab on a Chip.

Supplementary information

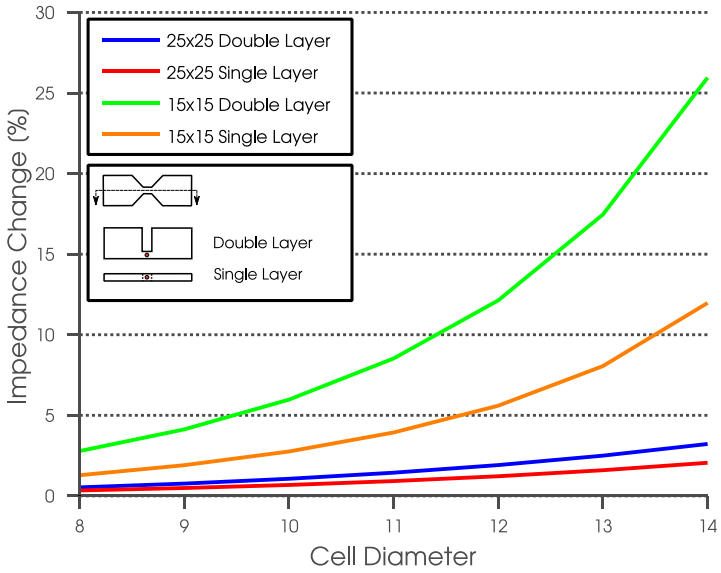

Fig. 1 Impedance simulation results based on the Coulter principle for varying constriction channel geometries and cells sizes. Both 15 μm×15 μm and 25 μm×25 μm constriction channel geometries are larger than WBC diameters to ensure that the channel does not physically deform cells during measurement. The importance of multiple channel heights (single vs. double layered) is shown in the overall curvature of each plot. This exhibits the ability to distinguish between different cell sizes based on impedance changes.

$$\gamma = \left(\frac{1}{d_r} - 1\right), \beta = \frac{1}{d_r}, \text{ where } 0 < d_r < 1$$

(1) $$R_B = \gamma R_{b,1}$$

(2) $$\gamma R_{b,1} + \beta R_m + \gamma R_{w,1} = \frac{V}{i_B}$$

(3) $$\gamma R_{w,1} + \gamma R_{b,2} - R_j = \frac{V}{i_B}$$

$$\vdots$$

(4) $$\gamma R_{b,n} + \beta R_m + \gamma R_{w,n} = \frac{V}{i_B}$$

(5) $$\gamma R_{w,n} + \gamma R_{b,n+1} - R_j = \frac{V}{i_B}$$

(6) $$\gamma R_{b,n} + \beta \left(R_m + \frac{R_i + R_c}{R_c}\right) = \frac{V}{i_B}$$

Fig. 2 Electrical equations derived using the fluidic analogous circuit model. *V*, *i* and *R* are electrical analogues representing *pressure*, *volumetric flow* and *fluidic resistance*, respectively. Subscripts denote fluidic resistors in various modules from $j = 1$ to the *n*-th serial module: (B: blood, b: buffer, w: waste, l: lysis, q: quench, m: mixing and c: constriction). $\boldsymbol{d_r}$ denotes the desired dilution ratio, $\boldsymbol{\gamma}$ and $\boldsymbol{\beta}$ are summarized variables dependent on $\boldsymbol{d_r}$. Resistor values are iteratively resolved.

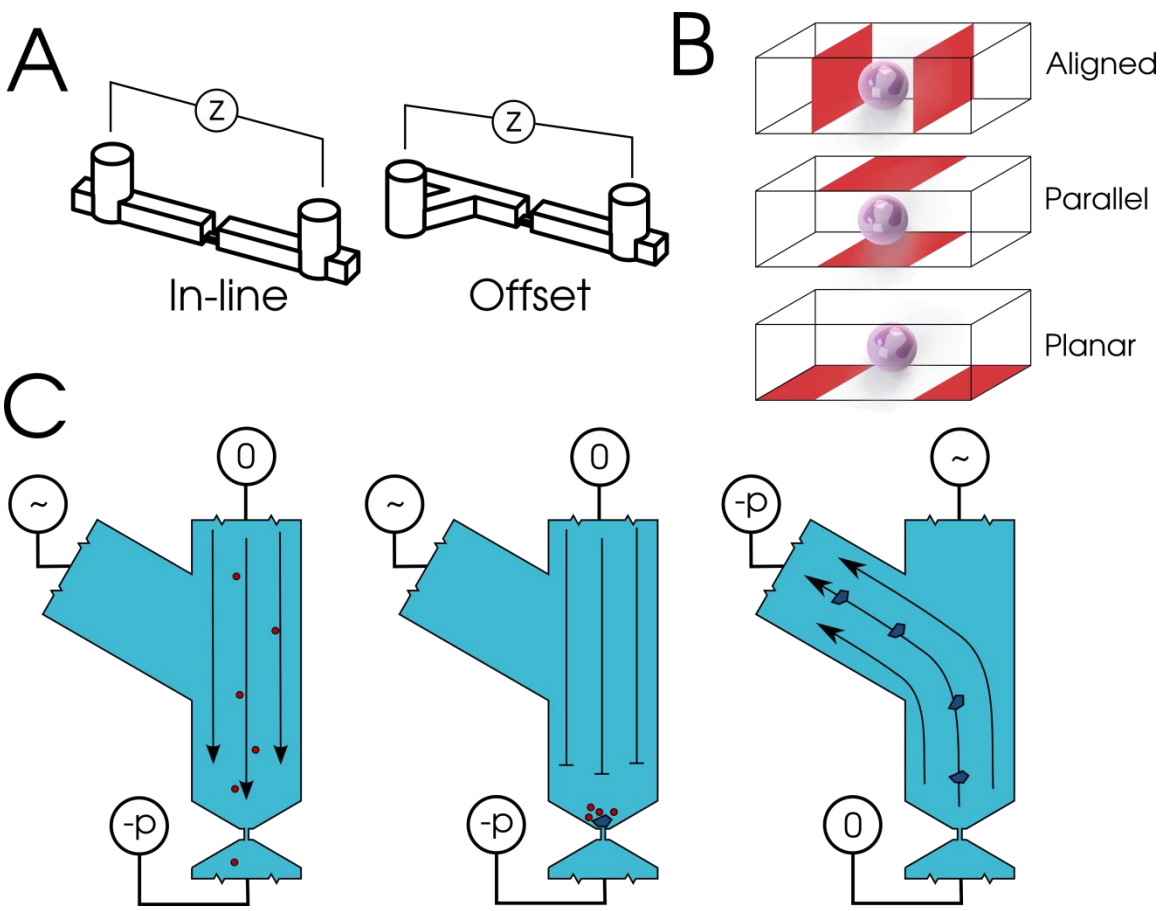

Fig. 3 Electrode configurations. (A) Schematic highlighting difference between conventional plug in electrodes (in-line) and our reconfigured electrode placement. (B) Different electrode configurations for measuring single cells in flow. (C) Unclogging mechanism. Left: normal operation of the device with indicated pressure drops. Center: debris occluded constriction channel and restricts all flow. Right: applied pressure is adjusted to redirect flow into the electrode region and all debris is cleared.

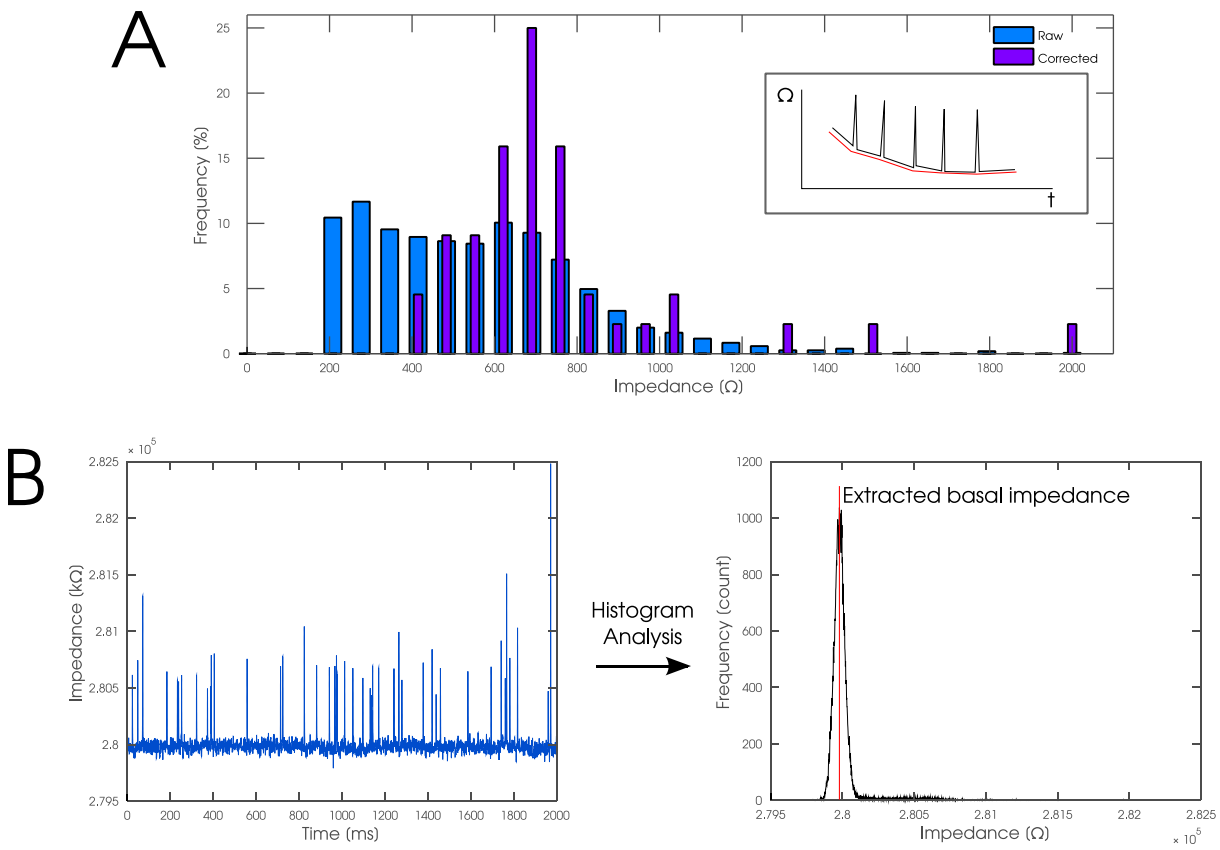

Fig. 4 Signal processing approach. (A) RBC size histograms for raw and post baseline correction. Raw histogram (blue) has large number of cells at lower electrical volumes due to mis-identification. Size histogram from baseline correction shows improvement in size accuracy and produces expected RBC distribution. Inset: summary of baseline correction algorithm. Low ordered polynomial (red) is fitted and subtracted from raw data to eliminate baseline trends. (B) Basal impedance calculation algorithm. Left: raw windowed data segment after baseline correction. Right: histogram of raw impedance data with extracted basal impedance.

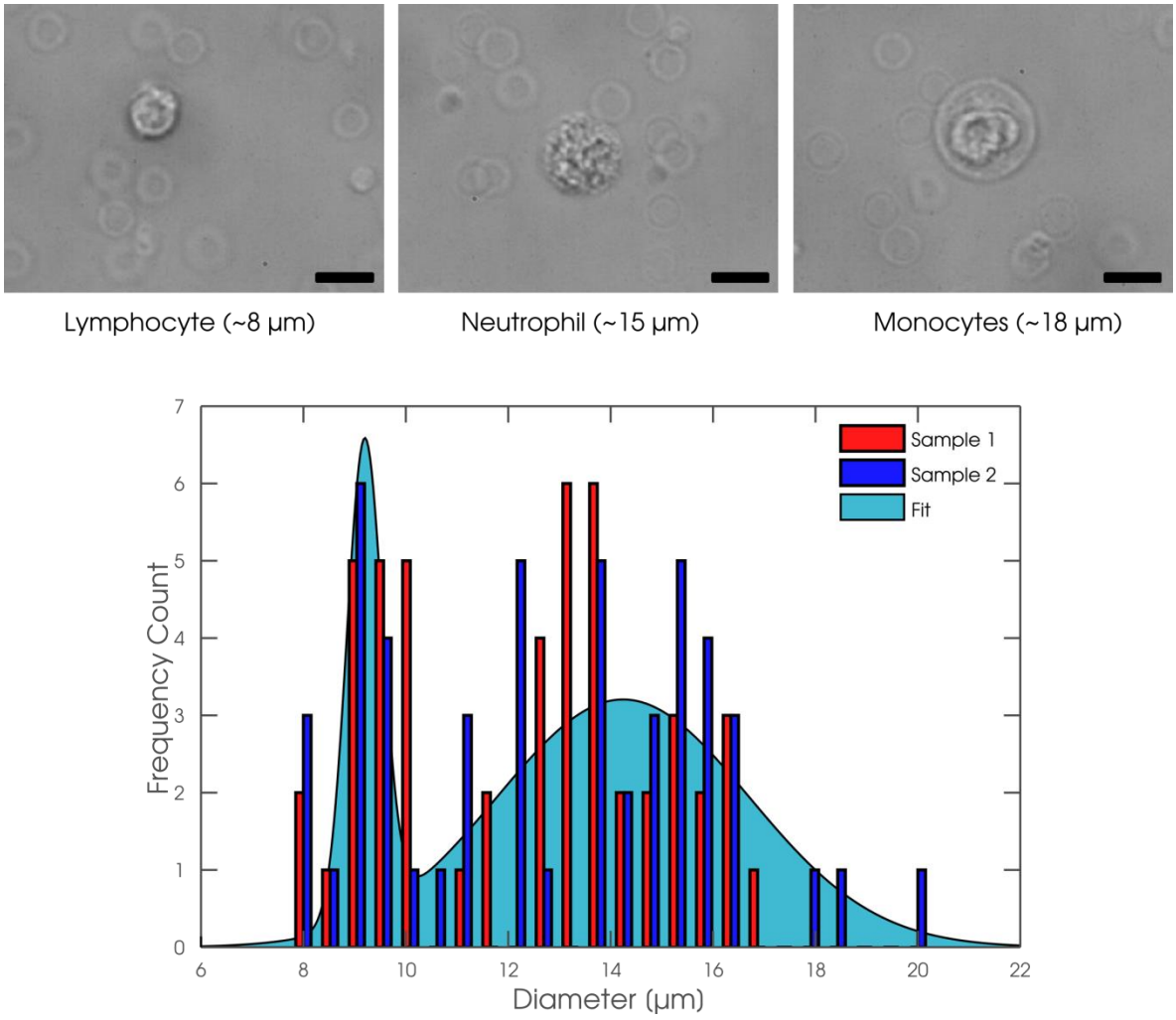

Fig. 5 Top: microscopy imaging confirmation of cell diameter difference of different WBC subtypes. Scale bars are 15 µm. Bottom: cell diameter histogram from microscopy imaging measurements from two separate samples (*n*=40).